Fracture behavior of polycaprolactone/clay nanocomposites

LN Ludueña, A Stocchi and VA Alvarez

Abstract

The effect of clay-organo modifier on the thermal and mechanical properties and fracture behaviors of pure polycaprolactone (PCL) and 5 wt% PCL/clay nanocomposites were studied. The different materials were prepared by melt intercalation. It was demonstrated by X-ray diffractometry, differential scanning calorimetry, tensile, and fracture tests that the addition of modified nanoclays affected significantly the final properties of the materials. The optimal combination of properties was achieved with the PCL reinforced with 5 wt% of C30B obtaining improvements of 17% in the Young's modulus and 1500% in the specific essential fracture work.

Keywords

Biodegradable polymer, clay, nanocomposite, fracture

Introduction

Packaging is the biggest industry of polymer processing. Food industry is its principal customer. Despite environmental problems, polymer packaging European market is increasing in about millions of tons per year. Foreseeing future laws about reducing the weight and volume of these products, cheap and biodegradable polymeric products are receiving growing attention.[1] Polycaprolactone (PCL) belongs to this class of synthetic biodegradable polymers. PCL is linear, hydrophobic, and partially crystalline polyester that can be slowly consumed by microorganisms.[2] It can be processed using conventional plastics machinery[2,3] and its properties make it suitable for a number of potential applications from agricultural usage to biomedical devices.[4] The main limitation of PCL is its weak rigidity and low fracture toughness which can be greatly enhanced by the dispersion of nanometer-size particles. This kind of materials are called nanocomposites and have the interesting characteristic of the mechanical properties;[3] the barrier properties;[5] the thermal properties;[6] and some others such as the resistance to flammability[7] and resistance to water adsorption,[8] can be greatly enhanced with the addition of a small amount of filler (usually less than 10 wt%). Some nanocomposites may achieve significant and simultaneous improvements in stiffness, fracture toughness and these characteristics could be of particular importance in several industries.[9]

One kind of these nanometer-size reinforcements is the montmorillonite, which is a cheap and environmental-friendly layered silicate whose interlayer ions can be changed by organ-ions in order to produce an increment in the interlayer spacing and to improve the polymer/clay compatibility. These improvements allow the dispersion of clay platelets to be easier. As far as totally dispersion of the clay platelets (exfoliation) is achieved, the reinforcement phase is more effective.[10] Instead of fully exfoliated structures, intercalated structures (the silicate layers are intercalated between polymer chains) or a mixture of both, are generally achieved.[11]

Several works dealing with the dispersion of organo-modified and natural montmorillonite inside PCL by melt blending can be found in various literatures.[1,3,12–18] Other methods involves in situ synthesis of PCL/clay masterbatches in supercritical carbon dioxide[19] and the host–guest chemistry.[20] Also, some authors deal with the clay dispersion in the PCL/clay in foams.[21] From these works it can be concluded that the organo-modified montmorillonite leads to better dispersed PCL/clay nanocomposites.

Research Institute of Material Science and Technology (INTEMA), Composite Materials Group (CoMP), Engineering Faculty, National University of Mar del Plata, Argentina

Corresponding author:
LN Ludueña, Research Institute of Material Science and Technology (INTEMA), Composite Materials Group (CoMP), Engineering Faculty, National University of Mar del Plata, Juan B. Justo 4302 Mar del Plata, B7608FDQ, Argentina.
Email: luduenaunmdp@gmail.com

This result demonstrates that the chemical compatibility between the clay and the matrix is the key to homogenously disperse these kinds of nanoparticles in the polymer matrix. On the other hand, several authors[22–26] demonstrated that the clay organo-modifiers can be degraded during the melt blending process. Therefore, not only the clay/polymer compatibility but also the processing stability of the clay organo-modifier should be the key to obtain well dispersed polymer/organo-modified clay nanocomposites by melt blending. In order to verify this hypothesis, in a previous work[12] we studied effect of natural montmorillonite and five commercial organo-modified clays on the final performance of PCL-based nanocomposites prepared by melt mixing. Nanocomposites with 5 wt.% of each clay were prepared by double-screw extrusion at the same processing conditions where it was found that the commercial clay named Cloisite 20 A (C20A) was the organo-modified clay with the best balance between processing stability and chemical compatibility with the PCL. Thus, PCL/C20A nanocomposites showed the best clay dispersion degree and, hence, the best mechanical performance.

Nano-/micro-sized inorganic particles as filler to enhance polymer toughness have been reported and well documented.[27] The effects of different particle size, distribution, and dispersion inside the polymer matrix have been studied and reviewed.[28] The fracture behavior of polymer composites is generally associated with the interfacial area between the matrix and the reinforcement. Good interfacial properties allow a good load transfer from the polymer matrix to the reinforcement. On the other hand, if the interface is weak the mechanical behavior will be poor. For nanocomposites, very large surfaces with low volumes allow to have considerable effects at very low concentrations of reinforcement. This interphase region has strong chemical matrix–reinforcement interactions, promoting remarkable changes in mechanical performance of the composite.

The aim of this work is to improve the fracture behavior of PCL/clay nanocomposites and correlate the obtained result with their morphology and tensile mechanical properties.

Experimental

Materials

The matrix used in this work was a commercial polycaprolactone, PCL (Mn 80,000, Mn/Mw < 2, glass transition −60°C, melting temperature 60°C, density 1.145 g/mL at 25°C), provided by Sigma Aldrich. Several Cloisite clays commercially purchased from Southern Clay Products Inc., USA, were used as nanofillers. They were used as received. The characteristics of the clays are shown in Table 1.
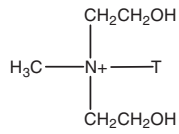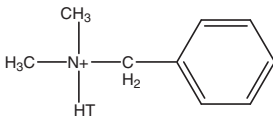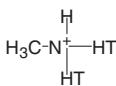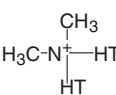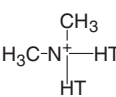
Preparation of nanocomposites

Neat matrix (PCL) and nanocomposites with 5.0 wt% of clay were prepared by melt-intercalation in a Brabender type mixer. Nanocomposites were named 5Clay_Name (i.e. 5C30B is the nanocomposite with 5 wt% of Cloisite 30B). Mixing temperature was 100°C, screws rotation speed was 150 r/min, and mixing time was 10 min. Then, 0.5 mm thick sheets were prepared by compression molding in a hydraulic press following the next steps: 10 min at 100°C; $0\,kg/cm^2 \rightarrow 10\,min$ at 100°C; $50\,kg/cm^2 \rightarrow$ water cooling of molds at $50\,kg/cm^2 \rightarrow$ mold opening.

Characterization of matrix and nanocomposites

Thermogravimetric analysis (TGA). This was carried out in a Shimadzu TGA-50 from 30°C to 1000°C at 10°C/min. Tests in nitrogen atmosphere were done to calculate the clay content inside the nanocomposites, which was in the range of 5.0 ± 0.6 wt% for all materials. These values were calculated from the residual mass of the composites at 900°C correcting for the residual mass of the neat matrix and for the weight loss of the neat clays at the same temperature. The weight loss of the neat clays at 900°C is mainly composed of water and/or organic content. These calculations were carried out assuming that thermal degradation of the clay organo-modifiers did not take place during the intercalation process. This assumption is supported by results obtained in a previous study.[29] In that work, we characterized the thermal degradation of the clays by TGA as shown in Table 1. Isothermal tests were carried out at temperatures close to those used in the processing conditions reported in the previous section (120–140–160–180°C) for 3 and 30 min. The maximum heating rate allowed by the equipment was used to reach each temperature. These tests were conducted in air to simulate more realistically the environment during processing operations. It was demonstrated that the less stable organo-modifier of the clays shown in Table 1 starts to thermally degrade at temperatures above 160°C. These results suggest that the organo-modifiers of the clays were not thermally degraded at the processing temperatures used in this work.

X-ray diffractometry (XRD). XRD patterns of C20A and nanocomposites were recorded by a PW1710 diffractometer equipped with an X-ray generator ($\lambda = 0.15401$ nm). Samples were scanned in 2θ ranges from 1.5° to 60° by a step of 0.035°. The interlayer spacing of the clays was calculated before and after mixing by means of the Bragg's law. The values were named as $d_{001}^{initial}$ (as-received clays) and d_{001}^{final} (clay inside the compression molded samples).

Table 1. Characteristics of the clays used as nanofillers.

Clay	Organic modifier[a]	Modifier concentration (mEq/100 g clay)	Specific gravity, ρ_p (g/cm^3)
Montmorillonite (CNa+)	None	–	2.86
Closite 30B (C30B)		90	1.98
Closite 10A (C10A)		125	1.90
Cloisite 93A (C93A)		90	1.88
Cloisite 20A (C20A)		95	1.77
Cloisite 15A (C15A)		125	1.66

[a]HT is hydrogenated tallow (~65% C18; ~30% C16; ~5% C14).

Differential scanning calorimetry (DSC). Tests were performed in a Shimadzu DSC-50 from 25°C to 100°C at a heating rate of 10°C/min under nitrogen (ASTM D3417-83). The degree of crystallinity was calculated from the following equation

$$X_{cr}(\%) = \frac{\Delta H_f}{w_{PCL} \times \Delta H_{100}} \times 100 \qquad (1)$$

where ΔH_f is the experimental heat of fusion, w_{PCL} the PCL weight fraction, and ΔH_{100} is the heat of fusion of 100% crystalline PCL and its value is 136.1 J/g.[30]

Tensile tests. It was performed in a universal testing machine Instron 4467 at a constant crosshead speed of 50 mm/min. Before tests, all specimens were preconditioned at 65% RH (relative humidity) and room temperature.

Fracture tests. Fracture characterization was carried out on mode I double edge-notched tensile (DENT) specimens cut from 0.5 mm films (nominal width W was 15 mm and nominal length S was 70 mm), at a crosshead speed of 1.5 mm/min. Sharp notches were introduced by sliding a fresh razor blade having an on-edge tip radius of 0.13 mm. Series of 10 specimens were tested. Energy release rate values were obtained from these tests.

Theoretical background

Essential work of fracture approach

The essential work of fracture (EWF) approach is a methodology that works well for very ductile polymer composites.[31] This approach was first proposed for plane stress ductile metal fractures and later applied to polymers.[32] The experimental simplicity is one of the most attractive features of the EWF method. For this approach, measurement of the ligament length before testing is only needed instead of

measuring the crack extension as required in the J-integral method.[33]

The aim of the EWF approach is to separate the work performed in the fracture process zone, W_e, from the total work of fracture, W_f, and that in ductile polymers is often dominated by the work of plastic deformation, W_p.

$$W_f = W_e + W_p \qquad (2)$$

The EWF method makes use of the fact that the essential work and the plastic work scale differently for a given specimen thickness (B) and ligament length (l)

$$W_f = w_e lB + w_p \beta l^2 B \qquad (3)$$

where β is the shape factor, and w_e and w_p are the specific essential work of fracture and the specific nonessential work of fracture, respectively. According to the known literature, EWF parameters depend on different physical factors[34] like thermal aging, molecular weight, annealing, and test conditions such as temperature, deformation rate, loading mode, etc.[35–37]

By dividing W_f by the ligament area l, it is possible to obtain the specific total work w_f that can be expressed as

$$w_f = w_e + w_p \beta l \qquad (4)$$

If the entire specimen ligament deforms plastically before fracture initiation, then the specific essential work can be found by testing different ligament lengths and extrapolating the specific total work of fracture to zero ligament length.

The EWF method is valid for polymers under certain conditions. The first condition is full ligament yielding prior to crack propagation and self-similarity between load and displacement curves. Other important requirement is the minimum ligament length: it has to be at least three times greater than the specimen thickness. Moreover, the stress criterion suggested by Clutton[38] i.e. $0.9\sigma_m < \sigma_{max} < 1.1\sigma_m$, where $\sigma_{max} = F/L$; F is the maximum load in a DENT specimen, l is the total ligament length, and σ_m is the mean of σ_{max} values that have to be satisfied. The EWF method cannot be used if a material does not fulfil the conditions mentioned above.

In recent years, the EWF method has been extensively applied to polymers[36] and there is a draft standard of the European Structural Integrity Society (ESIS).[38] The EWF method delivers a single fracture parameter that is representative of crack propagation. The EWF approach can also be used for plane strain fracture J_{Ic} either obtained from slow strain rate tests[39,40] or impact tests.[41]

Results and discussions

Nanocomposite morphology (XRD)

The final properties of nanocomposites are determined by both the reinforcement content and its dispersion degree inside the matrix.[3] The morphology of the nanocomposites was analyzed by means of the interlayer spacing of the clay inside the nanocomposites (d_{001}^{final}).

Figure 1 and Table 2 resumes the results, also including the $d_{001}^{initial}$ values. The $d_{001}^{initial}$ parameter is important because it is expected that as $d_{001}^{initial}$ increases, polymer chains have more space to intercalate, obtaining a better dispersed nanocomposite.

The highest values of $d_{001}^{initial}$ and d_{001}^{final} were found for the C15A clay and 5C15A, respectively. On the other hand, the 5C30B nanocomposite was the only case for which the d_{001}^{final} value could not be calculated due to the disappearance of the diffraction peak, as shown in Figure 1. There are two possible reasons for this behavior, the structure of the nanocomposite is intercalated but the value of d_{001}^{final} is so high that it could not be calculated by means of the equipment used, or the nanocomposite does not present ordering anymore (exfoliated structure). Therefore, it can be concluded that the 5C30B nanocomposite showed the highest clay dispersion degree inside the matrix.

Mechanical properties

Table 3 shows the mechanical properties of the neat matrix and the nanocomposites. The crystallinity degree of the materials is also included in this table.

It was observed that all clays enhanced the Young's modulus of the neat matrix, while the tensile strength and the elongation at break remained almost constant. Highest Young's modulus of the PCL/clay nanocomposites is expected as a function of the clay dispersion degree.[42] In this work, a clear correlation of the Young's modulus with the morphology of the nanocomposites was not obtained. The crystallinity degree of the matrix also affects the mechanical performance of the nanocomposites.[43] It can be observed in Table 3 that this parameter was around 70% for all materials without showing significant variations after clay incorporation.

Mode I EWF analysis

Typical load–displacement curves for the neat PCL and nanocomposites are shown in Figure 2. The curves corresponding to only two nanocomposites were plotted for the sake of clarity. Similar shape of the curves was observed for all materials. A marked load drop is seen after reaching the maximum load corresponding to the full ligament shielding[31,44] followed by a more
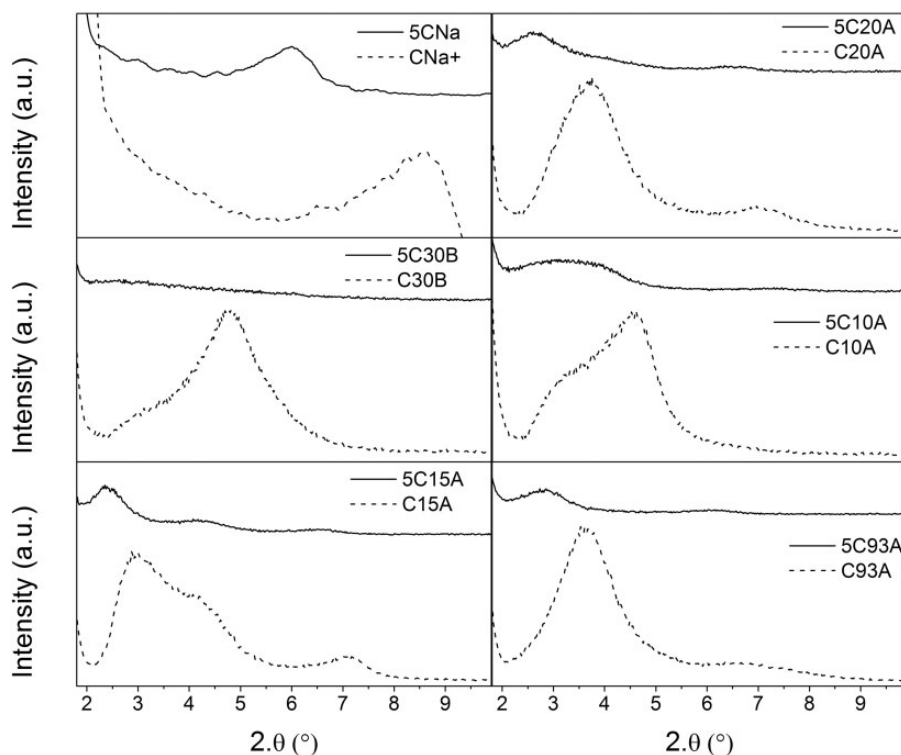
Figure 1. XRD diffractograms of the nanocomposites.

Table 2. Results from XRD tests.

Material	$d_{001}^{initial}$ (Å)	d_{001}^{final} (Å)
5CNa	10.2	14.5
5C30B	18.4	No peak
5C10A	19.3	27.5
5C93A	24.0	31.6
5C20A	23.9	33.6
5C15A	29.5	36.9

gradual drop corresponding to necking and tearing of the ligament.[45]

The 5C30B composite showed the higher load for ligament yielding and the less prominent load drop leading to higher fracture energy. On the other hand, the neat PCL matrix showed similar maximum load but a marked load drop, leading to lower fracture properties. All the other studied nanocomposites had an intermediate behavior between the neat matrix and the 5C30B reinforced composite.

The toughening mechanisms for micro-sized particle reinforced composites have been studied for many years and there are several publications available in literatures.[46–49] However, the nano-particles lead to different toughening mechanisms than microparticles and the traditional mechanisms may not be present.[50]

Work of fracture plots for the investigated nanocomposites are depicted in Figure 3.

A good linear correlation was found for all the materials studied in this work. The values of W_e were calculated from the interception of the linear fit extrapolated to zero ligament length, and are presented in Figure 4. Figure 5 shows the β_{wp} values calculated as the slope of the linear fit.

There are several factors that affect the performance of nanoclays as reinforcement.[50] In cases of good compatibility, the formation of an interphase between the filler and matrix increases the stiffness and toughness as a function of the clay dispersion degree. All the compatibilized clay reinforced nanocomposites showed increased properties in comparison with the untreated clay. This result is in accordance with other authors who found in some cases that the chemical treatment of the reinforcements increases the fracture toughness.[51,52] The EWF results indicate that the C30B nanoclay chemical modification was the most efficient, which is in accordance with the clay dispersion degree of this material. The nanocomposites reinforced with C15A and C20A showed significant differences on the EWF results even having organo-modifiers with the same chemical structure. The dissimilar behavior can be attributed to the higher concentration of the organo-modifier between the silicate layers of C15A which increases the $d_{001}^{initial}$ promoting the easier intercalation

Table 3. Mechanical properties of the neat matrix and their nanocomposites.

Material	E (MPa)	σ (MPa)	ε (%)	X_{cr} (%)
PCL	299 ± 18	14.9 ± 0.4	872 ± 144	72.1 ± 0.2
5CNa	314 ± 18	15.1 ± 0.5	895 ± 13	69.2 ± 0.4
5C30B	351 ± 22	14.7 ± 0.7	796 ± 181	67.8 ± 0.1
5C10A	410 ± 36	15.3 ± 1.2	826 ± 103	70.1 ± 0.1
5C93A	371 ± 31	15.1 ± 0.5	856 ± 16	68.9 ± 0.3
5C20A	375 ± 6	14.8 ± 0.7	882 ± 58	69.7 ± 0.2
5C15A	369 ± 18	15.1 ± 0.3	808 ± 79	70.7 ± 0.1

E = Young's modulus, σ = tensile strength, ε = elongation at break, X_{cr} = crystallinity degree.
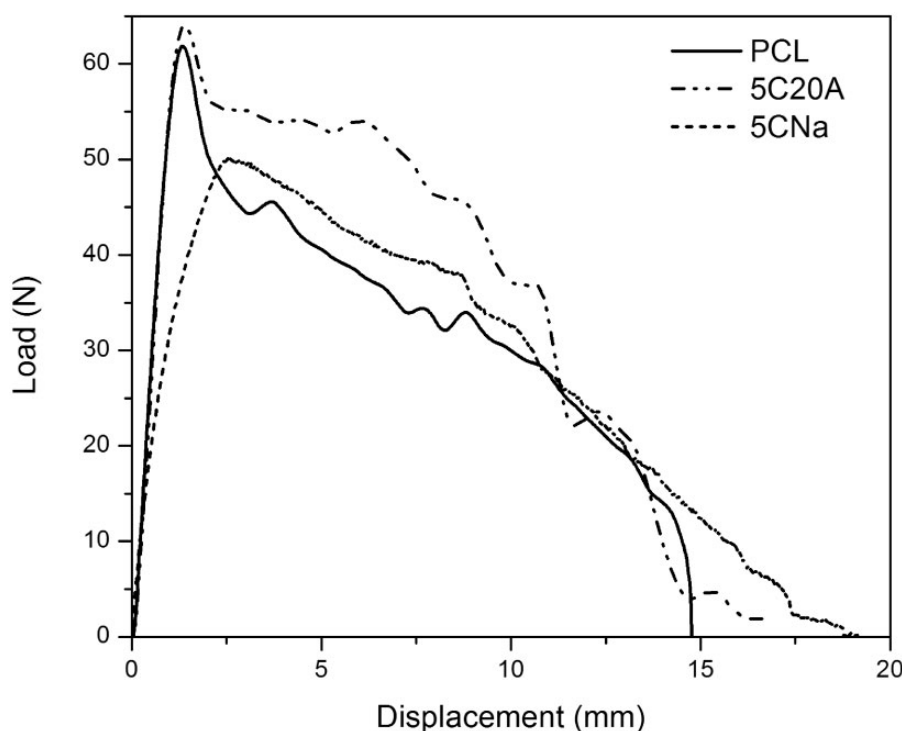
Figure 2. Load–displacement curves for the neat matrix and nanocomposites.

of the polymer chains. The higher clay dispersion degree of the 5C15A nanocomposite demonstrated by XRD confirms this hypothesis. The case of the 5C93A nanocomposite cannot be explained by this analysis. Lower clay dispersion degree was seen for 5C93A than the 5C20A nanocomposite but higher W_e values than 5C15A. Both the molecular weight and concentration of the organo-modifier between the silicate layers of C93A are lower than that of C15A and C20A. Nanocomposites having the same or similar clay dispersion degree but higher concentration of silicate layers, which is achieved with low concentrations of low molecular weight organo-modifiers, should show improved reinforced efficiency. Therefore, EWF

behavior results from a balance between clay dispersion degree and concentration of silicate layers.

It can be noted that in all cases the particle reinforcement lead to an improvement of specific work of fracture. As mentioned before, the 5C30B nanocomposite showed an improvement of 1500% in the specific work of fracture. The lower contribution was found for the 5CNa unmodified clay with an improvement of 46%. These results are in accordance with the morphology found and the measured tensile properties of the nanocomposites.

It can be seen that the addition of 5 wt% of C10A, C15A, and C93A had a positive effect on energy consumption for plastic deformation. On the other hand,
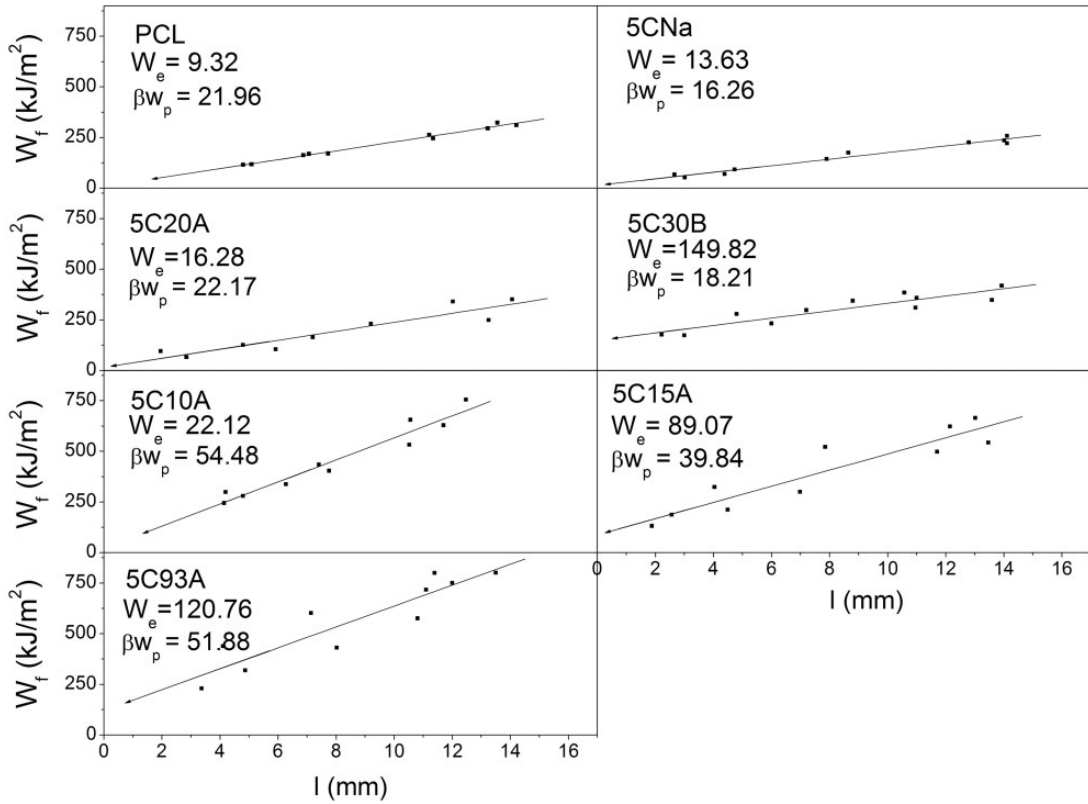
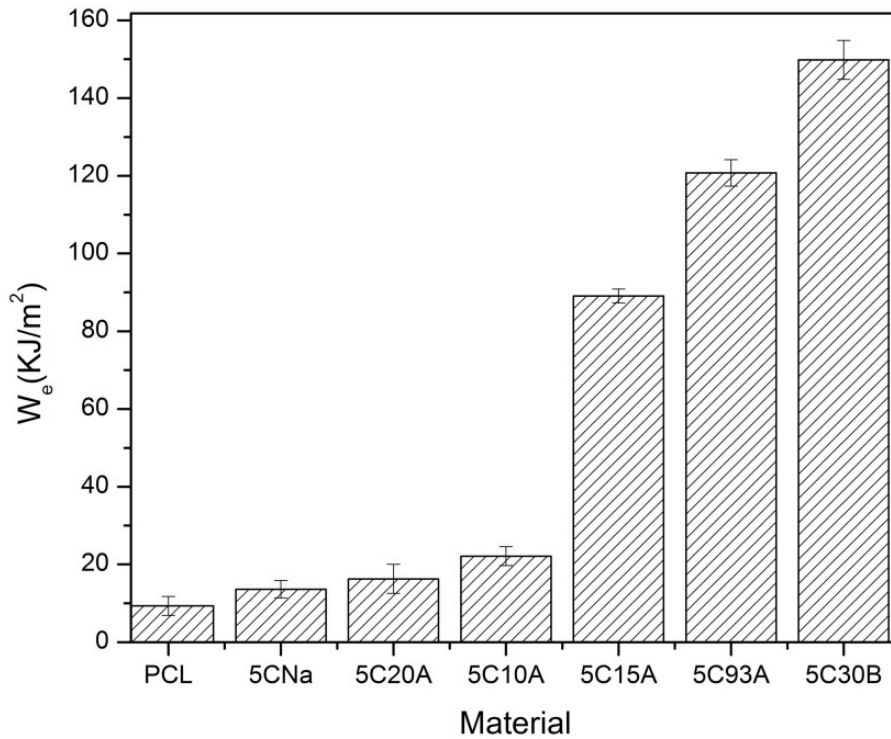**Figure 3.** Work of fracture plots for the neat matrix and nanocomposites.

Figure 4. Specific essential fracture work W_e for the neat matrix and nanocomposites.
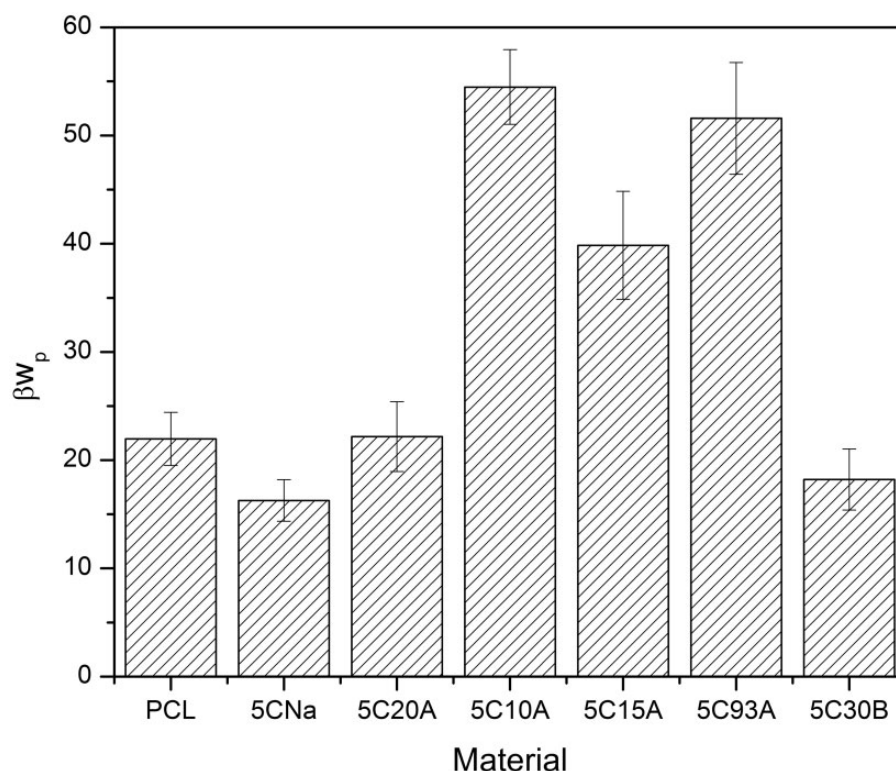
Figure 5. Specific plastic work of fracture values for the neat matrix and nanocomposites.

lower values of β_{wp} in comparison with that of the neat matrix were found for 5CNa and 5C30B nanocomposites suggesting less plastic energy absorbed in plastic deformation during the fracture process.

Essentially, the increment W_e for all reinforced nanocomposites indicates that the incorporation of nanoclays induced an increase in resistance to crack initiation.[53] On the other hand, the values of β_{wp} showed an increased crack propagation resistance for the 5C10A, 5C15A, and 5C93A but a decrease in this parameter for 5CNa and 5C30B, respectively. This can be mainly attributed to the different compatibilities of each clay with the matrix and the processing resistance of the clay organo-modifiers. In addition, it should be noted that the organo-modified clays have modifier contents ranging from 90 to 125 mEq/100 g clay. This means that these reinforcements have lower contents of silicate platelets than the sodium montmorillonite. The silicate platelets are the reinforcing phase so, the optimization of the balance between clay dispersion degree and the silicate platelet content is the key factor for polymer reinforcement.

Conclusions

The mechanical and fracture behavior of polycaprolactone/clay nanocomposites prepared by melt blending was studied in this work. All clays used enhanced the mechanical and fracture behavior of the PCL. The optimal combination of properties was achieved with the PCL reinforced with 5 wt% of C30B obtaining improvements of 17% in the Young's modulus and 1500% in the specific essential fracture work. On the other hand, there was not a clear trend between the clay dispersion degree and the mechanical and fracture behavior. This result could be attributed to the fact that organo-modifiers enhance clay dispersion degree inside the polymer matrix but reduce the clay platelets content, which are the reinforcing phase, per clay mass. Thus, low contents of nonmodified sodium clays could maintain an acceptable clay dispersion degree inside the PCL matrix with higher clay platelets contents per clay mass. The balance between both situations should always be optimized in order to find the optimal mechanical behavior.

Science and Technology (ANPCyT) [Fonarsec FSNano004], and the National University of Mar del Plata (UNMdP) [15G327].

References

1. Lepoittevin B, Devalckenaere M, Pantoustier N, et al. Poly([var epsilon]-caprolactone)/clay nanocomposites prepared by melt intercalation: mechanical, thermal and rheological properties. *Polymer* 2002; 43: 4017–4023.

2. Kunioka M, Ninomiya F and Funabashi M. Novel evaluation method of biodegradabilities for oil-based polycaprolactone by naturally occurring radiocarbon-14 concentration using accelerator mass spectrometry based on ISO 14855-2 in controlled compost. *Polym Degrad Stab* 2007; 92: 1279–1288.

3. Ludueña LN, Alvarez VA and Vazquez A. Processing and microstructure of PCL/clay nanocomposites. *Mater Sci Eng A* 2007; 460–461: 121–129.

4. Dubois P, Jacobs C, Jerome R, et al. Macromolecular engineering of polylactones and polylactides. 4. Mechanism and kinetics of lactide homopolymerization by aluminum isopropoxide. *Macromolecules* 1991; 24: 2266–2270.

5. Messersmith PB and Giannelis EP. Synthesis and barrier properties of poly(ε-caprolactone)-layered silicate nanocomposites. *J Polym Sci Part A: Polym Chem* 1995; 33: 1047–1057.

6. Kojima Y, Usuki A, Kawasumi M, et al. Mechanical properties of nylon 6-clay hybrid. *J Mater Res* 1993; 8: 1185–1189.

7. Gilman JW, Jackson CL, Morgan AB, et al. Flammability properties of polymer–layered-silicate nanocomposites. Polypropylene and polystyrene nanocomposites. *Chem Mater* 2000; 12: 1866–1873.

8. Gorrasi G, Tortora M, Vittoria V, et al. Vapor barrier properties of polycaprolactone montmorillonite nanocomposites: Effect of clay dispersion. *Polymer* 2003; 44: 2271–2279.

9. Ahmed J, Varshney SK, Zhang J-X, et al. Effect of high pressure treatment on thermal properties of polylactides. *J Food Eng* 2009; 93: 308–312.

10. Ranade A, Nayak K, Fairbrother D, et al. Maleated and non-maleated polyethylene-montmorillonite layered silicate blown films: Creep, dispersion and crystallinity. *Polymer* 2005; 46: 7323–7333.

11. Fischer H. Polymer nanocomposites: From fundamental research to specific applications. *Mater Sci Eng C* 2003; 23: 763–772.

12. Ludueña LN, Kenny JM, Vázquez A, et al. Effect of clay organic modifier on the final performance of PCL/clay nanocomposites. *Mater Sci Eng A* 2011; 529: 215–223.

13. Janigová I, Lednický F, Mošková DJ, et al. Nanocomposites with biodegradable polycaprolactone matrix. *Macromol Sympos* 2011; 301: 1–8.

14. Di Y, Iannace S, Di Maio E, et al. Nanocomposites by melt intercalation based on polycaprolactone and organoclay. *J Polym Sci Part B: Polym Phys* 2003; 41: 670–678.

15. Homminga D, Goderis B, Dolbnya I, et al. Crystallization behavior of polymer/montmorillonite nanocomposites. Part II. Intercalated poly(ε-caprolactone)/montmorillonite nanocomposites. *Polymer* 2006; 47: 1620–1629.

16. Homminga D, Goderis B, Hoffman S, et al. Influence of shear flow on the preparation of polymer layered silicate nanocomposites. *Polymer* 2005; 46: 9941–9954.

17. Lepoittevin B, Pantoustier N, Devalckenaere M, et al. Polymer/layered silicate nanocomposites by combined intercalative polymerization and melt intercalation: A masterbatch process. *Polymer* 2003; 44: 2033–2040.

18. Peponi L, Puglia D, Torre L, et al. Processing of nanostructured polymers and advanced polymeric based nanocomposites. *Mater Sci Eng R* 2014; 85: 1–46.

19. Urbanczyk L, Calberg C, Stassin F, et al. Synthesis of PCL/clay masterbatches in supercritical carbon dioxide. *Polymer* 2008; 49: 3979–3986.

20. Arslan M, Tasdelen MA, Uyar T, et al. Poly(epsilon caprolactone)/clay nanocomposites via host–guest chemistry. *Eur Polym J* 2015; 71: 259–267.

21. Tsimpliaraki A, Tsivintzelis I, Marras SI, et al. Foaming of PCL/clay nanocomposites with supercritical CO2 mixtures: The effect of nanocomposite fabrication route on the clay dispersion and the final porous structure. *J Supercrit Fluids* 2013; 81: 86–91.

22. VanderHart DL, Asano A and Gilman JW. NMR measurements related to clay-dispersion quality and organic-modifier stability in nylon-6/clay nanocomposites. *Macromolecules* 2001; 34: 3819–3822.

23. VanderHart DL, Asano A and Gilman JW. Solid-state NMR investigation of paramagnetic nylon-6 clay nanocomposites. 2. Measurement of clay dispersion, crystal stratification, and stability of organic modifiers. *Chem Mater* 2001; 13: 3796–3809.

24. Alexandre M and Dubois P. Polymer-layered silicate nanocomposites: Preparation, properties and uses of a new class of materials. *Mater Sci Eng R* 2000; 28: 1–63.

25. Xie W, Gao Z, Liu K, et al. Thermal characterization of organically modified montmorillonite. *Thermochim Acta* 2001; 367–368: 339–350.

26. Xie W, Gao Z, Pan WP, et al. Thermal degradation chemistry of alkyl quaternary ammonium Montmorillonite. *Chem Mater* 2001; 13: 2979–2990.

27. Meng B, Tao J, Deng J, et al. Toughening of polylactide with higher loading of nano-titania particles coated by poly(ε-caprolactone). *Mater Lett* 2011; 65: 729–732.

28. Fu S-Y, Feng X-Q, Lauke B, et al. Effects of particle size, particle/matrix interface adhesion and particle loading on mechanical properties of particulate–polymer composites. *Compos Part B: Eng* 2008; 39: 933–961.

29. Ludueña LN, Kenny JM, Vázquez A, et al. Effect of clay organic modifier on the final performance of PCL/clay nanocomposites. *Mater Sci Eng A* 2011; 529: 215–223.

30. Yam WY, Ismail J, Kammer HW, et al. Polymer blends of poly(ϵ-caprolactone) and poly(vinyl methyl ether) – thermal properties and morphology. *Polymer* 1999; 40: 5545–5552.

31. Karger-Kocsis J, Czigány T and Moskala EJ. Thickness dependence of work of fracture parameters of an amorphous copolyester. *Polymer* 1997; 38: 4587–4593.

32. Cotterell B and Reddel JK. The essential work of plane stress ductile fracture. *Int J Fract* 1977; 13: 267–277.

33. Poon WKY, Ching ECY, Cheng CY, et al. Measurement of plane stress essential work of fracture (EWF) for polymer films: Effects of gripping and notching methodology. *Polym Test* 2001; 20: 395–401.

34. Tuba F, Oláh L and Nagy P. Characterization of reactively compatibilized poly(d,l-lactide)/poly(ε-caprolactone) biodegradable blends by essential work of fracture method. *Eng Fract Mech* 2011; 78: 3123–3133.

35. Bárány T, Ronkay F, Karger-Kocsis J, et al. In-plane and out-of-plane fracture toughness of physically aged polyesters as assessed by the essential work of fracture (EWF) method. *Int J Fract* 2005; 135: 251–265.

36. Bárány T, Czigány T and Karger-Kocsis J. Application of the essential work of fracture (EWF) concept for polymers, related blends and composites: A review. *Prog Polym Sci* 2010; 35: 1257–1287.

37. Kuno T, Yamagishi Y, Kawamura T, et al. Deformation mechanism under essential work of fracture process in polycyclo-olefin materials. *Express Polym Lett* 2008; 2: 404–412.

38. Clutton E. Essential work of fracture. In: Moore AP and Williams JG (eds) *European structural integrity society*. New York: Elsevier, 2001, pp.177–195.

39. Luna P, Bernal C, Cisilino A, et al. The application of the essential work of fracture methodology to the plane strain fracture of ABS 3-point bend specimens. *Polymer* 2003; 44: 1145–1150.

40. Wu J and Mai Y-W. The essential fracture work concept for toughness measurement of ductile polymers. *Polym Eng Sci* 1996; 36: 2275–2288.

41. Wu J, Mai Y and Cotterell B. Fracture toughness and fracture mechanisms of PBT/PC/IM blend. *J Mater Sci* 1993; 28: 3373–3384.

42. Ludueña LN, Vázquez A and Alvarez VA. Effect of the type of clay organo-modifier on the morphology, thermal/mechanical/impact/barrier properties and biodegradation in

soil of polycaprolactone/clay nanocomposites. *J Appl Polym Sci* 2013; 128: 2648–2657.

43. Ludueña LN, Vazquez A and Alvarez VA. Crystallization of polycaprolactone-clay nanocomposites. *J Appl Polym Sci* 2008; 109: 3148–3156.

44. Ching ECY, Poon WKY, Li RKY, et al. Effect of strain rate on the fracture toughness of some ductile polymers using the essential work of fracture (EWF) approach. *Polym Eng Sci* 2000; 40: 2558–2568.

45. Zhao H and Li RKY. Fracture behaviour of poly(ether ether ketone) films with different thicknesses. *Mech Mater* 2006; 38: 100–110.

46. Norman DA and Robertson RE. Rigid-particle toughening of glassy polymers. *Polymer* 2003; 44: 2351–2362.

47. Lee J and Yee AF. Role of inherent matrix toughness on fracture of glass bead filled epoxies. *Polymer* 2000; 41: 8375–8385.

48. Lee J and Yee AF. Inorganic particle toughening I: micro-mechanical deformations in the fracture of glass bead filled epoxies. *Polymer* 2001; 42: 577–588.

49. Móczó J and Pukánszky B. Polymer micro and nanocomposites: Structure, interactions, properties. *J Ind Eng Chem* 2008; 14: 535–563.

50. Sun L, Gibson RF, Gordaninejad F, et al. Energy absorption capability of nanocomposites: A review. *Compos Sci Technol* 2009; 69: 2392–2409.

51. Sternstein SS and Zhu A-J. Reinforcement mechanism of nanofilled polymer melts as elucidated by nonlinear viscoelastic behavior. *Macromolecules* 2002; 35: 7262–7273.

52. Kalgaonkar RA and Jog JP. Effects of modifier concentration on structure and viscoelastic properties of copolyester/clay nanocomposites. *J Macromol Sci Part B* 2005; 43: 421–436.

53. Dayma N, Kumar S, Das D, et al. Melt-mixed PA-6/LDPE-g-MA/nanoclay ternary nanocomposite: Micromechanisms from post-yield fracture kinetics and strain field analysis. *Mater Chem Phys* 2013; 142: 640–650.